[논 문] 한국재료학회지
Korean J. Mater. Res.
Vol. 25, No. 12 (2015)
http://dx.doi.org/10.3740/MRSK.2015.25.12.690

Fatigue Crack-Tip Stress Mapping Using Neutron Diffraction

Gyudong Choi[1], Min-Ho Lee[1], E-Wen Huang[2], Wanchuck Woo[3] and Soo Yeol Lee[1†]

[1]Department of Materials Science and Engineering, Chungnam National University, Daejeon 305-764, Korea
[2]Department of Materials Science and Engineering, National Chiao Tung University, Hsinchu, 300, Taiwan (R.O.C.)
[3]Neutron Science Division, Korea Atomic Energy Research Institute, Daejeon 305-353, Korea

(Received October 7, 2015 : Revised October 23, 2015 : Accepted October 26, 2015)

Abstract Fatigue crack growth experiments were carried out on a 304 L stainless steel compact-tension(CT) specimen under load control mode. Neutron diffraction was employed to quantitatively measure the residual strains/stresses and the evolution of stress fields in the vicinity of a propagating fatigue-crack tip. Three principal stress components (i.e. crack growth, crack opening, and through-thickness direction stresses) were examined in-situ under loading as a function of distance from the crack tip along the crack-propagation path. The stress/strain fields, measured both at the mid-thickness and near the surface of the CT specimen, were compared. The results show that much higher compressive residual stress fields developed in front of the crack tip near the surface than developed at the mid-thickness area. The change of the stresses ahead of the crack tip under loading is more significant at the mid-thickness area than it is near the surface.

Key words fatigue, crack growth, stress field, stainless steel, neutron diffraction.

1. Introduction

Fatigue is a form of failure that occurs in many engineering components subjected to dynamic and fluctuating stress.[1)] Preventing and predicting fatigue-damage failure are therefore crucial for the improvement in the lifetimes of numerous components and structures.[2)] Since fatigue crack growth behavior is governed by a localized plastic deformation at the propagating crack tip, the residual stresses and their interaction with an external stress near the crack tip become important to characterize the local deformation behavior. It is generally known that compressive residual stresses are found to decrease the crack propagation rates, while tensile residual stresses produce the opposite effect.[3)] Thus, the accurate determination of the residual stresses and their influence on the applied stresses are critical for a fundamental understanding of the fatigue crack growth behavior. Various nondestructive diffraction techniques, e.g. laboratory X-ray diffraction, high-energy synchrotron X-ray diffraction and tomography, and neutron diffraction, have been used to investigate the fatigue crack deformation and failure behavior by directly measuring internal stress/strain fields in the bulk fatigued specimen.[4-14)]

In this work, neutron diffraction was employed to investigate the distribution of residual stresses/strains and the evolution of the internal stresses in the vicinity of a fatigue crack tip during fatigue crack growth of 304 L stainless steel compact-tension(CT) specimen. The three-orthogonal-direction crack-tip stress fields, which are obtained from the directly-measured three-orthogonal-direction strain components without the assumptions of plane strain or plane stress conditions, are examined as a function of distance from the crack tip with 1-mm spatial resolution of neutron beam along the crack-propagation direction. The residual and internal stress/strain fields measured at the mid-thickness and near the surface are compared.

2. Experimental Procedures

2.1 Materials and fatigue testing

A 304 L stainless steel with a single-phase face-centered-cubic structure was used for this study. This alloy has a yield strength of 241 MPa, an ultimate tensile strength of 586 MPa, and elongation of 55 percent at room temperature. A nominal chemical composition of this alloy is

†Corresponding author
E-Mail : sylee2012@cnu.ac.kr (S. Y. Lee, Chungnam Nat'l Univ.)

© Materials Research Society of Korea, All rights reserved.
This is an Open-Access article distributed under the terms of the Creative Commons Attribution Non-Commercial License (http://creativecommons.org/licenses/by-nc/3.0) which permits unrestricted non-commercial use, distribution, and reproduction in any medium, provided the original work is properly cited.

Table 1. Chemical composition of 304 L stainless steel [wt.%].

Chemical composition	C	Mn	P	S	Si	Cr	Ni	N	Fe
wt.%	0.03	2	0.045	0.03	0.75	18-20	8-12	0.1	balance

shown in Table 1.

The fatigue crack growth(FCG) experiment was carried out on the 304 L stainless steel compact-tension(CT) specimen, prepared by the American Society of Testing and Materials(ASTM) Standard E647-99. Before the FCG experiment, the CT sample was pre-cracked approximately 1.27 mm, then constant-amplitude fatigue crack growth test was performed under a load control mode with the following conditions [P_{max} = 7400 N, P_{min} = 740 N, the load ratio R = 0.1, and frequency = 10 Hz]. The crack length was measured by a compliance method using a crack-opening-displacement gauge. When the crack length reached 18 mm, the fatigue crack growth test was stopped, and then the fatigued sample was used for residual strain/stress mapping and in-situ internal stress mapping, respectively.

2.2 Neutron diffraction measurements

The spatially-resolved neutron diffraction strain mapping was performed on the Residual Stress Instrument(RSI) at the High-flux Advanced Neutron Application Reactor (HANARO) of the Korea Atomic Energy Research Institute(KAERI). Three orthogonal direction strain components [crack-growth(ε_x), crack-opening(ε_y), and through-thickness(ε_z) direction strains] were measured as a function of distance from the crack tip along the crack-growth direction. The schematics of sample geometry and measurement positions are shown in Fig. 1.

Two sets of stress/strain mapping were conducted: The first set of mapping was performed along a center line of the CT specimen; the second set of mapping was conducted at 2.4 mm above the center line, which is very close to the surface of the sample. The strain measurement positions are from −3 mm behind the crack tip to 10 mm ahead of the crack tip for the both sets of mapping.

In-situ neutron diffraction was performed to examine the evolution of the internal stress fields around the crack tip under applied loads. The three orthogonal direction lattice strains were measured at the four loading levels (i.e., 0P_{max}(zero load), 0.3P_{max}, 0.6P_{max}, and P_{max}), as the sample was in situ deformed. The wavelength of 1.46 Å was chosen from the Si (200) monochromator. The (311) diffraction peak was recorded in a detector centered on a diffraction angle of $2\theta = 84^{o}$. The experimental set-up for the in-situ neutron diffraction measurements are shown in Fig. 2.

The peak position was determined using the Gaussian fitting of the {311} diffraction peak in all three directional strain component(crack-growth, crack-opening, and through-thickness component) measurements. The lattice strains were then calculated using the following equation.

$$\varepsilon = (d - d_0) / d_0 = -cot\ \theta(\theta - \theta_0) \quad (1)$$

where the d_0 is the stress-free d-spacing, d is the interplanar spacing under the stressed condition, the θ_0 and θ are the diffraction angles for the stress-free and stressed

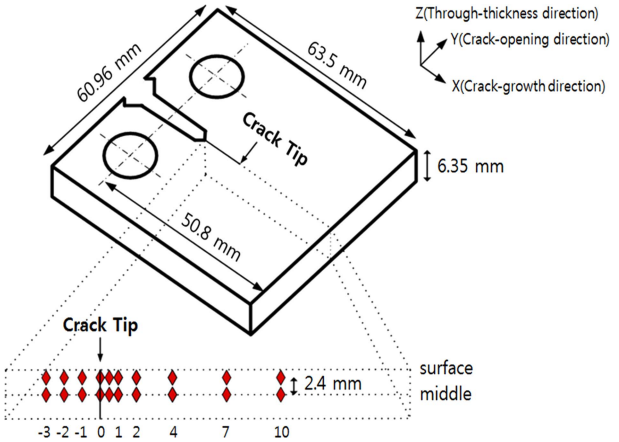

Fig. 1. Geometry of the CT specimen and lattice strain measurement positions by neutron diffraction. The mapping was performed along the crack-growth direction(X-direction) at the two different locations; one is in the middle of the specimen, the other is 2.4 mm above the center along the through-thickness direction(near the surface).

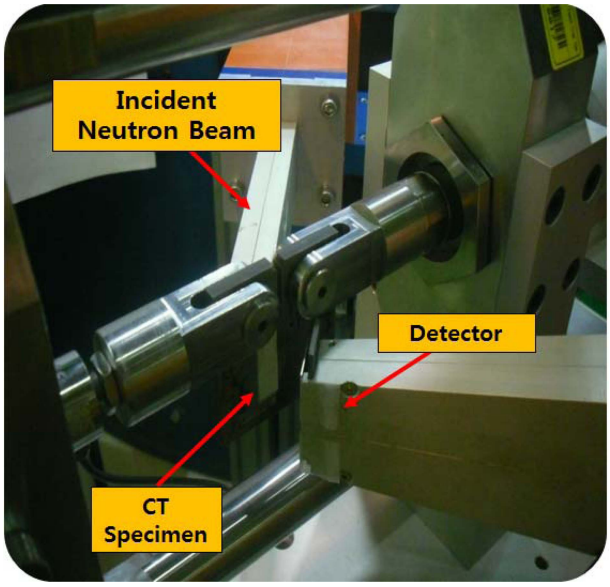

Fig. 2. Experimental set-up for in-situ neutron diffraction.

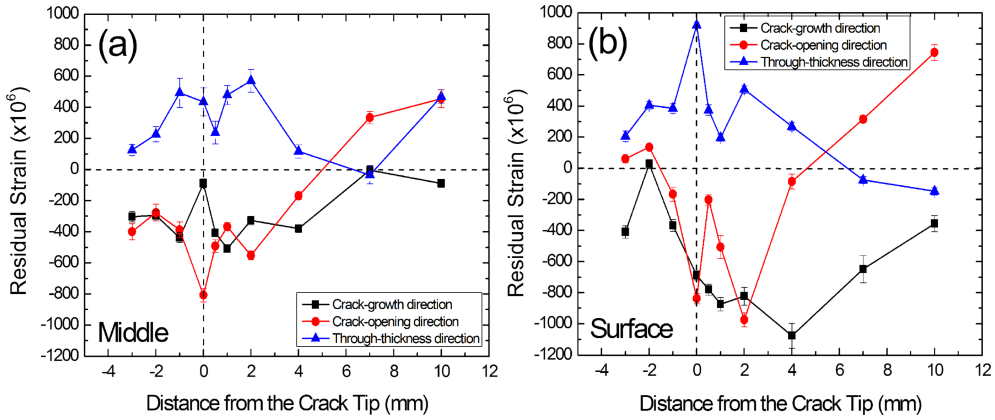

Fig. 3. Residual strain distributions for the crack-growth, crack-opening, and through-thickness directions (a) at the mid-thickness and (b) near the surface of the CT specimen.

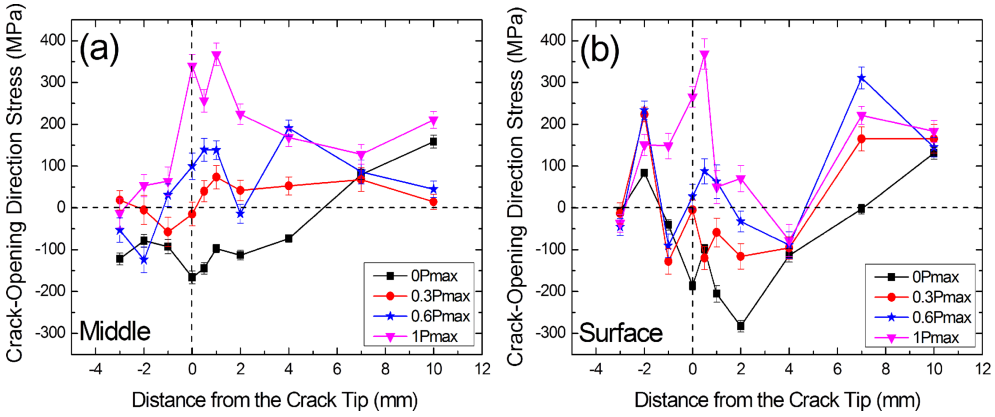

Fig. 4. Evolution of the stress fields near the crack tip under an applied load (a) at the mid-thickness and (b) near the surface.

condition at each position around the crack tip, respectively. The stress-free reference lattice spacing was measured 10 mm away from the corner of the annealed CT specimen. Three stress components, σ_i [$i = x$, y, and z, corresponding to crack-growth, crack-opening, and through-thickness directions, respectively], were calculated from the three measured principal strain components under loading using the following equation:

$$\sigma_i = \frac{E}{1+\nu}\left[\varepsilon_i + \frac{\nu}{1-2\nu}(\varepsilon_x + \varepsilon_y + \varepsilon_z)\right] \quad (2)$$

where E(= 183.5 GPa) is the Young's modulus and ν(= 0.31) is the Poisson's ratio.

3. Results and Discussion

Fig. 3 shows the residual strain distributions around a propagating crack tip at the mid-thickness(Fig. 3a) and near the surface(Fig. 3b) of the CT specimen in the three orthogonal directions(crack-growth, crack-opening, and through-thickness direction). In the crack-growth-direction strain measurement, the compressive residual strains with a maximum of −500 με(at 1-mm location) were observed at the mid-thickness of the sample(Fig. 3a), whereas much larger compressive residual strains, especially in the locations ahead of the crack tip, were developed near the surface of the sample(Fig. 3b). The maximum compressive residual strains near the surface were about −1080 με at the 4-mm location in front of the crack tip. Overall, the compressive residual stresses near the surface were more pronounced than those at the mid-thickness.

In the crack-opening direction strain component, the compressive residual strains with a maximum of ~ −800 με(at the crack tip) were observed in the locations of −3~ 5 mm at the mid-thickness of the sample(Fig. 3a). A double-valley shape was observed at the surface of the sample: maximum compressive residual strains of ~ −830 με and −980 με were observed at the crack tip and 2-mm location, respectively. Overall, higher crack-opening-direction residual strains were observed at the surface of the sample. In contrast, tensile residual stresses in the through-thickness direction were developed both at the mid-thick-

ness and near the surface. The highest tensile residual stress of ~920 με was observed at the crack tip near the surface.

The development of the stress fields at the mid-thickness(Fig. 4a) and near the surface(Fig. 4b) was examined in situ under loading, as shown in Fig. 4. The residual stresses at the surface were more significant than those at the mid-thickness, as similarly observed in the strain distribution in Fig. 3. The largest compressive residual stresses of ~ −285 MPa were observed at 2-mm location ahead of the crack tip at the surface of the fatigued sample.

In Fig. 4a, as the applied load increases, stresses of ~140 MPa increased behind the crack tip, while much larger increase of the stresses was observed ahead of the crack tip(0~7 mm) due to higher stress concentration right in front of the crack tip. The largest change of the stresses was ~500 MPa at the crack tip, and the change of the stresses becomes smaller as the location is far away from the crack tip.

In Fig. 4b, while no significant change of stresses was observed behind the crack tip at −3 and −2 mm locations, the stresses increased significantly at the locations of −1~4 mm near the crack tip. The largest increase of stresses was ~470 MPa at the 0.5-mm location near the surface of the sample(Fig. 4b). Overall, the change of the stresses ahead of the crack tip under loading, which might be related to the effective stress influencing the driving force of crack growth, is more significant at the mid-thickness than near the surface. Recognizing that the crack propagation rate at the mid-thickness is faster than that at the surface, it is thought that the higher effective stresses in front of the crack tip at the mid-thickness might be closely related to the faster crack growth rate in the middle of the specimen. The current results suggest that the discrepancy of the evolution of the stress fields at the mid-thickness and near the surface of the sample might be associated with the different stress transfer phenomena at the crack tip, related to the crack-tip driving force, along the through-thickness direction. Further analysis is under investigation.

4. Conclusions

Neutron diffraction was used to measure the residual strain fields in the vicinity of the crack tip at the mid-thickness and near the surface. The compressive residual strains were observed around the crack tip in the crack-growth and crack-opening direction both at the mid-thickness and near the surface. However, the compressive residual strains ahead of the crack tip near the surface were much more significant than those at the mid-thickness. The residual strains near the crack tip in the through-thickness direction were tensile both at the mid-thickness and near the surface. The evolution of the stress fields at the mid-thickness and near the surface was investigated in situ under loading. While the stresses at the mid-thickness of the CT specimen evolved behind the crack tip as well as up to 7 mm in front of the crack tip, no significant change of stresses was observed behind the crack tip(−3 ~ −2 mm location) in case of the surface mapping. It seems that near the surface, most of the stresses are concentrated at −1~4 mm location around the crack tip during loading. The change of the stresses ahead of the crack tip under loading at the mid-thickness is more significant than that near the surface.

Acknowledgement

This work was supported by a research fund of the Chungnam National University.

References

1. S. Suresh, Fatigue of Materials, 2nd ed., Cambridge University Press, New York (1998).
2. P. J. Withers, Rep. Prog. Phys., **70**, 2211 (2007).
3. J. D. Almer, J. B. Cohen and R. A. Winholtz, Metall. Mater. Trans. A, **29**, 2127 (1998).
4. J. E. Allison, Fracture mechanics, STP 677, Philadelphia, PA: ASTM, 550 (1979).
5. M. N. James, D. G. Hattingh, D. J. Hughes, L. W. Wei, E. A. Patterson and J. Q. Da Fonseca, Fatigue Fract. Eng. Mater. Struct., **27**, 609 (2004).
6. M. C. Croft, N. M. Jisrawi, Z. Zhong, R. L. Holtz, K. Sadananda, J. R. Skaritka and T. Tsakalakos, Int. J. Fatigue, **29**, 1726 (2007).
7. A. Steuwer, M. Rahman, A. Shterenlikht, M. E. Fitzpatrick, L. Edwards and P. J. Withers, Acta Mater., **58**, 4039 (2010).
8. A. J. Allen, M. T. Hutchings, C. G. Windsor and C. Andreani, Adv. Phys., **34**, 445 (1985).
9. M. T. Hutchings, C. A. Hippsley and V. Rainey, Mater. Res. Soc. Sympos. Proc., **166**, 317 (1990).
10. S. Y. Lee, R. I. Barabash, J. S. Chung, P. K. Liaw, H. Choo, Y. Sun, C. Fan, L. Li, D. W. Brown and G. E. Ice, Metall. Mater. Trans. A, **39**, 3164 (2008).
11. S. Y. Lee, H. Choo, P. K. Liaw, E. C. Oliver and A. M. Paradowska, Scripta Mater., **60**, 866 (2009).
12. S. Y. Lee, P. K. Liaw, H. Choo and R. B. Rogge, Acta Mater., **59**, 485 (2011).
13. S. Y. Lee, H. Choo, P. K. Liaw, K. An and C. R. Hubbard, Acta Mater., **59**, 495 (2011).
14. S. Y. Lee, E. W. Huang, W. Wu, P. K. Liaw and A. M. Paradowska, Mater. Charact., **79**, 7 (2013).